Contents lists available at ScienceDirect

Science of the Total Environment

journal homepage: www.elsevier.com

Combined magnetic, chemical and morphoscopic analyses on lichens from a complex anthropic context in Rome, Italy

Aldo Winkler [a, *], Chiara Caricchi [a], Maurizio Guidotti [b], Malgorzata Owczarek [b], Patrizia Macrì [a], Manuela Nazzari [a], Antonio Amoroso [b], Alessandro Di Giosa [b], Stefano Listrani [b]

[a] *Istituto Nazionale di Geofisica e Vulcanologia, Via di Vigna Murata 605, 00143 Rome, Italy*
[b] *ARPA Lazio, Regional Environmental Protection Agency, Rome and Rieti, Italy*

ARTICLE INFO

Article history:
Received 17 May 2019
Received in revised form 28 June 2019
Accepted 30 June 2019
Available online xxx

Editor: Elena Paoletti

Keywords:
Air pollution
Magnetic biomonitoring
Heavy metals
Particulate matter (PM)
Environmental magnetism
Lichens

ABSTRACT

Native and transplanted lichens were analyzed as bioaccumulators of airborne particulate matter (PM) in two selected areas of an eastern district of Rome, Italy, where frequent fraudulent fires are set to recover metals, mostly copper, from waste electrical and electronic equipment (WEEE). The presence of native lichens was scarce, due to the drought of spring-summer 2017, thus, sampling was extended to a neighboring site for toughening the dataset to a similar context. The magnetic analyses revealed intense properties connected to the anthropic complexity of the area, where industrial, traffic and arson-related dusts are continuously emitted and bio-accumulated. Magnetic parameters were compared to the chemical determinations, leading to significant linear correlations between the concentration dependent magnetic parameters (susceptibility, saturation magnetization and saturation remanence) and the concentration of heavy metals (among which copper, chrome, lead and zinc). Moreover, selected magnetic particles were chemically and morphologically characterized by a Scanning Electron Microscope and Energy Dispersion System microanalyses. Magnetic particles resulted incorporated into the lichens' tissues and their composition, morphology and grain size strongly supported their anthropogenic, mostly combustion-related, origin. Even if, given the complexity of the area, it was not feasible to fully discriminate the multiple anthropogenic sources, magnetic biomonitoring of lichens, especially when combined with microtextural and compositional analyses, confirmed to be an excellent methodology for a rapid characterization of environmental pollution.

1. Introduction

Particulate matter (PM) consists of a mixture of solid particles and liquid droplets of organic and inorganic substances suspended in the air.

According to WHO (2014, 2016), PM is associated with a broad spectrum of acute and chronic illness, such as lung cancer and cardiovascular diseases. Fine and ultra-fine particles, with the diameter ranging from nanometric to 10 μm, are the most dangerous, since they can penetrate and persist deep inside the lungs, affecting different organs, as well as several cell types. Abundant presence of magnetite nanoparticles, formed by combustion and/or friction-derived, which are common in urban airborne PM, has been recently found even in the human brain, where they can enter directly through the olfactory nerve (Maher et al., 2016).

Instrumental monitoring of PM requires expensive stations, power availability and continuous maintenance; beside, biomonitoring with cryptogams (in particular, lichens and mosses) has frequently been used for high resolution detection of the emission sources and the distribution patterns of various airborne persistent pollutants (e.g. heavy metals, polycyclic aromatic hydrocarbons−PAHs, dioxins, furans; Augusto et al., 2013, 2015; Guidotti et al., 2000, 2003; Owczarek et al., 2001, Bargagli and Mikhailova, 2002; Lucadamo et al., 2015; Nascimbene et al., 2014; Protano et al., 2014; Tretiach et al., 2007, 2011). Where autochthonous cryptogams are absent or rare (e.g. urban centers and indoor), transplants allow the application of a high-density sampling (Kodnik et al., 2015) and may help in determining the temporal patterns of airborne pollutants (Branquinho et al., 2008; Frati et al., 2005; Guidotti et al., 2009; Protano et al., 2017).

In the study area, *Xanthoria parietina* was the available native lichen: it is a foliose species that usually grows from rural to man-made areas on various substrates: barks of several tree species, rocks, walls in cement, tiles, bricks, fiberglass, roofing; it is widely used in biomonitoring of airborne metals for its high tolerance to atmospheric pollution (Demiray et al., 2012).

For lichen transplants, fruticose species are usually preferred over foliose species (Brunialti and Frati, 2014), because they ensure greater biomass per lichen thallus, as well as easier cleaning and in-

* Corresponding author.
Email addresses: aldo.winkler@ingv.it (A. Winkler); chiara.caricchi@ingv.it (C. Caricchi); maurizio.guidotti@arpalazio.gov.it (M. Guidotti); malgorzata.owczarek@arpalazio.gov.it (M. Owczarek); patrizia.macri@ingv.it (P. Macrì); manuela.nazzari@ingv.it (M. Nazzari); antonio.amoroso@arpalazio.gov.it (A. Amoroso); alessandro.digiosa@arpalazio.gov.it (A. Di Giosa); stefano.listrani@arpalazio.gov.it (S. Listrani)

https://doi.org/10.1016/j.scitotenv.2019.06.526
0048-9697/

stallation, thus contextually reducing processing time and enhancing sample homogeneity (Wolterbeek and Bode, 1995).

The epiphytic fruticose lichen *Pseudevernia furfuracea*, selected for this study, is a frequently used biomonitor of heavy metals and PAHs (Gallo et al., 2014; Kodnik et al., 2015; Nascimbene et al., 2014; Tretiach et al., 2007; Tretiach et al., 2011). This lichen is relatively common, easy to identify, stress-tolerant, with a good resistance to transplantation (Tretiach et al., 2007), and morphologically prone to intercept PM (Tretiach et al., 2005). In general, *Pseudevernia furfuracea* is considered the main choice for this kind of studies.

It is frequently used in methodological studies (Adamo et al., 2007, 2008; Bari et al., 2001; Nascimbene et al., 2014; Vingiani et al., 2004) and applications (e.g. Tretiach et al., 2011); moreover, it is the only certified lichen (BCR 482, Quevauviller et al., 1996), and it was subjected to several histological (Rinino et al. 2005) and physiological studies (Tretiach et al., 2005).

A complementary method for analyzing and monitoring the airborne PM is the study of its magnetic properties. Aerosols may have remarkable magnetic properties related to the content of magnetite-like ferrimagnetic particles, often associated to heavy metals such as Cd, Cr, Zn (e. g. Flanders, 1994, Georgeaud et al., 1997; Hunt et al., 1984; Muxworthy et al., 2002; Sagnotti and Winkler, 2012; Hansard et al., 2012; Zhu et al., 2013; Jordanova et al., 2006; Lu et al., 2009) and even to mutagenic organic compounds (Morris et al., 1995). Magnetic analyses are cheap, sensitive, fast, and allow to discriminate between different sources of pollution, according to the magnetic grain size, as pointed out in urban and traffic related contexts (Sagnotti et al., 2009; Revuelta et al., 2014).

Magnetic biomonitoring of atmospheric pollution is a growing application in the field of environmental magnetism, since trace metals are incorporated into the magnetic particles that are deposited and accumulated on plant leaves and other biological receptors; biological surfaces, exposed to atmospheric pollution, accumulate magnetic particles over time, providing a record of location-specific, time-integrated air quality information (e.g. Hofman et al., 2017).

In magnetic biomonitoring studies, tree leaves (Maher et al., 2008; Mitchell et al., 2010; Moreno et al., 2003; Rai, 2013), barks (Böhm et al., 1998), mosses (Fabian et al., 2011; Vuković et al., 2015) and lichens (Chaparro et al., 2013; Paoli et al., 2017; Salo et al., 2012) have successfully been used as passive dust collectors, as well as in urban (e.g., Szönyi et al., 2008; Zhang et al., 2006), industrial (Hansard et al., 2011; Jordanova et al., 2010; Salo and Mäkinen, 2014; Zhang et al., 2008) and mixed land use areas (Kodnik et al., 2017), up to high density surveys in high-precipitation tropical cities and valleys (Mejía-Echeverry, 2018). Recently, the differences in net particle accumulation between 96 plant species were determined and expressed as leaf saturation isothermal remanent magnetization (Muhammad et al., 2019). Even if magnetic biomonitoring studies are more common for leaves, there is an increasing interest in lichens and mosses as PM interceptors and bioaccumulators (e.g. Chaparro et al., 2013, Fabian et al., 2011, Jordanova et al., 2010, Salo, 2014, Salo et al., 2012, Kodnik et al., 2017, Mejía-Echeverry et al., 2018), and, recently, even insects, crustaceans, mammal (of which human) tissues and spider webs are considered because their magnetic properties (Rachwał et al., 2018; Hofman et al., 2018).

Jordanova et al. (2010) found that lichens and mosses point the strongest contrast between clean and polluted environment; moreover, lichens introduce the possibility to apply the transplant technique in magnetic biomonitoring studies; suitable species are collected from pristine sites to be exposed in the target areas for assessing, in time and space, the air pollutant deposition and accumulation, and the consequent variation of the magnetic properties.

This study was conceived as a pilot multidisciplinary test to integrate the magnetic, chemical and morphoscopic properties of native and transplanted lichens sampled in an area subjected to several sources of atmospheric pollution, among which traffic and frequent fraudulent fires, which are causing growing concern in citizens living there and in public opinion. Arsons cause the production of harmful substances during uncontrolled combustion of plastics, waste and organic material. In this case, the uncontrolled combustions are set to free the metals, in particular Cu, contained in the waste, causing the formation of volatile organic material as well as metals, which are dispersed in the atmosphere and then fall back into adjacent soils, including green areas, often used as pastures for sheep. The testing hypothesis of this study was to verify that magnetic analyses are a rapid and sensitive tool for biomonitoring of airborne PM in multi-source pollution contexts, expanding what has been already tested in traffic and industrial conditions.

2. Methods

2.1. Lichen sampling and treatment

The first sampling campaign was carried out near a Roma camp around Via di Salone, in the easternmost side of Rome, where fraudulent fires are almost continuously set. A preliminary investigation, in July 6, 2017, revealed scarce presence of lichen populations in the affected area, taking into account the drought of spring-summer 2017. Despite this, the sampling of lichens was performed in July 25, 2017, following the guidelines for the use of epiphytic lichens as bioaccumulators of heavy metals (Bargagli and Nimis, 2002). Thus, lichens were collected from trunks with inclination within 10° from vertical and without evident signs of disturbance, at a sufficient height to neglect the soil influence. Four specimens of *Xanthoria parietina* native lichens, the only available species, were found and sampled from the trees of this area (Figs. 1a, b and 2a, Table 1).

To expand and compare the dataset, further sampling was carried out in July 14, 2017 in a 7 km far district, around Via Tiburtina and near Tivoli, affected by continuous rogues of waste material, in a similar context to the first area. Five more *Xanthoria parietina* samples were taken (Fig. 1a and c, Table 1).

Finally, a *Xanthoria parietina* control site has been sampled in Valle Oracola, an undisturbed rural area, near to the Regional Environmental Protection Agency (ARPA Lazio) chemical laboratory, about 60 km far from the investigated area, where undisturbed or pristine samples were not available.

Additionally, seven transplants of lichen *Pseudevernia furfuracea* have been exposed for 4 months in the Salone area, to expand the dataset and to investigate the change of magnetic properties from supposed pristine conditions (Fig. 1b). Pre-exposure specimens were originally sampled from the trees of a small wood at Monte Terminillo, 100 km far from the investigated area, in the same county of the *Xanthoria parietina* control sample in Valle Oracola.

The transplants have not been exposed in the Tiburtina area, since this study was specifically committed to ARPA Lazio, for analyzing the atmospheric pollution in the Salone area. The additional sampling in via Tiburtina was carried out for verifying that, when the man-made sources are similar, the results on native samples are uniform and do not depend on natural sources.

Practically, thalli of *Pseudevernia furfuracea* were inserted in the so-called "lichen bags", which are constituted by a plastic "not magnetic" frame that allows contact with the air, and can be subsequently fixed at a height of about two meters above the ground, in the site chosen for the study (Fig. 2b, c).

Fig. 1. a) Orthophotograph of Rome city, white square indicates the study area. CTR (Carta Tecnica Regionale) maps of sampling site locations: Via di Salone (b) and Via Tiburtina (c). Orthophotograph and CTR maps were downloaded from https://geoportale.regione.lazio.it/geoportale/.

Fig. 2. Sampling procedures: a) native lichens (Site S0); b, c) transplant exposure (Site TS1).

After the exposure period, only six samples were found, since one fell and was contaminated by soil (Table 2).

After sampling, most of the lichen material was prepared at the ARPA Lazio laboratory in Rieti for subsequent chemical analyses, or at Istituto Nazionale di Geofisica e Vulcanologia (INGV) laboratory in Rome for magnetic properties. Dead parts and foreign material (leaves, soil, talons of other lichens) were removed. For chemical determinations on native samples, only the last 2 mm external parts of several thalli collected in each site were analyzed, in order to take into account the same accumulation period for each sampling point. With regard to *Pseudevernia furfuracea* transplants, the chemical analyses were carried out on the entire homogenized sample. Sam-

Table 1
Location of the native lichens sampled around via di Salone and via Tiburtina.

Sampling sites		
Site name	Coordinates (LAT and LONG)	Description
Via di Salone		
S0	41° 55.098′ N 12° 38.340′ E	Inside a dismissed cement plant and near a wall facing the Roma camp sampled during the preliminary survey
S1	41° 55.206′ N 12° 38.118′ E	On the entrance wall of a dismissed cement plant
S2	41° 55.277′ N 12° 38.533′ E	On a canal bringing wastewater to Aniene river
S3	41° 54.822′ N 12° 37.014′ E	Near a Hotel facing the highway
Via Tiburtina		
T1	41° 56.882′ N 12° 42.572′ E	Adjacent to the motorway and to the urban agglomeration
T2	41° 56.791′ N 12° 42.631′ E	Denoting fire activity
T3	41° 56.938′ N 12° 43.623′ E	At the limit of a recent fire, from a tree partially damaged by the arson
T4	41° 56.448′ N 12° 43.110′ E	Along the road from the Martellona neighborhood to Tivoli Terme
T5	41° 56.449′ N 12° 42.717′ E	Near a car junkyard, in the innermost part of the area

Table 2
Location of the lichen transplants exposed around Via di Salone.

Transplant sites		
Site name	Coordinates (LAT and LONG)	Description
Via di Salone		
TS1	41° 54.917′ N 12° 38.130′ E	Near the Salone railway station
TS2	41° 55.206′ N 12° 38.118′ E	On the entrance wall of a dismissed cement plant (corresponding to native sample S1)
TS3	41° 55.098′ N 12° 38.340′ E	Inside a dismissed cement plant and near a wall facing the Roma camp (corresponding to native sample S0)
TS4	41° 55.086′ N 12° 38.358′ E	On a wall facing the Roma camp
TS5	41° 55.206′ N 12° 38.574′ E	On a canal bringing wastewater to Aniene river (corresponding to native sample S2)
TS7	41° 54.822′ N 12° 37.014′ E	Near a hotel facing the highway (corresponding to native sample S3).

ples were dried in air or in an oven at 40 °C for 48 h, to avoid any change of the magnetic mineralogy, and then shredded and/or homogenized, to be representative of the sampling site. For chemical determinations, all the samples, in duplicates, were prepared in the same day and then analyzed in the following day.

2.2. Magnetic characterization

Magnetic measurements were performed at the palaeomagnetic laboratory of the INGV. Fragments of lichens were put inside standard 8 cm^3 plastic cubes for the magnetic susceptibility (χ) measurements, and in pharmaceutical gel caps #4, of about 0.15 ml capacity, for the hysteresis properties investigations.

The magnetic susceptibility has been measured on AGICO MFK-1 Kappabridge and calculated by dividing the bulk values with the net weight of the samples, after subtraction of the empty holders.

The temperature dependency of the magnetic susceptibility was measured in free air, in the range 40 to 700 °C and back, with the AGICO MFK-1 Kappabridge equipped with a CS-3 furnace, and calculated after correction for the susceptibility of the empty furnace.

Gel cap samples vibrated in the Princeton Measurement Corporation Micromag 3900 Vibrating Sample Magnetometer (VSM) through a carbon fiber probe for defining the hysteresis loops. Small lichen fragments, irregularly dimensioned and shaped, were carefully pressed inside the caps to maximize the content and to prevent their movement during vibration. The coercive force (B_c), the saturation remanent magnetization (M_{rs}) and the saturation magnetization (M_s) were measured applying fields up to 1.0 T and determined after subtracting the high field paramagnetic linear trend. Mass-specific magnetization values for the concentration-dependent parameters were calculated dividing the magnetic moments for the net weight of the samples. The coercivity of remanence (B_{cr}) values were extrapolated from backfield remagnetization curves up to −1 T, following forward magnetization in a saturating +1 T field. On available samples, magnetic measurements were made on the same specimens prepared by both ARPA Lazio and INGV, to compare the results and to verify that they are mostly independent of shredding or homogenization, drying methods and cutting of the most external parts.

The magnetic grain-size of the PM accumulated by the lichens was investigated and compared to theoretical magnetite according to the hysteresis ratios M_{rs}/M_s vs. B_{cr}/B_c in the Day plot (Day et al., 1977; Dunlop, 2002a, 2002b).

First order reversal curves (FORCs; Pike et al., 1999; Roberts et al., 2000) were measured using the Micromag operating software; FORC diagrams were processed, smoothed and drawn with the FORCINEL Igor Pro routine (Harrison and Feinberg, 2008). FORCs were measured in steps of 2.5 mT, with 300 ms averaging time and maximum applied field being 0.5 T. The optimum smoothing factor was evaluated by FORCINEL software.

2.3. Chemical and morphoscopic characterization

The determination of metal content was conducted by graphite furnace atomic absorption spectrometry (AAS Varian Spectra AA 220Z). A total of 150 mg of finely chopped lichen was placed into a "Teflon bomb" with 7 ml of 63% HNO_3, 3 ml of 30% H_2O_2 and 0.2 ml of 40% HF. The container was closed with the appropriate Teflon screw cap and placed in an oven at 120 °C for 3 h. The con-

tainer was then removed from the oven and cooled at room temperature. The mixture was then transferred into a 50 ml glass flask, and bi-distilled water was then added to the flask. In order to eliminate the matrix effect, quantitative analyses were conducted using the standard addition method. The repeatability of the method was assessed by analyzing a reference standard material (BCR No. 482 – heavy metals in lichens) and repeating this procedure six times. The certificated values, recorded values, average recovery, relative standard deviations (RSD) and limits of quantification (LOQ) for each metal are reported in Table 1s.

The Pollution Load Index (PLI) has been obtained, for each site (i), from the concentration factors (CF), that are obtained by dividing the concentration of n metals for the background values which, in this case, refer to the control for native samples and to pre-exposure for transplants. The most recent background values for Italy, from Cecconi et al., 2019, have not been used for calculating the CFs, since they do not include Fe and Mn; Hg has been excluded from the computation, since it was not measured in transplants.

Thus, site specific PLI are calculated as (Tomlinson et al., 1980):

$$PLIi = (CF1i \times CF2i \times CF3i \times \ldots \times CFni)\hat{}1/n$$

Linear models for correlating the concentration dependent magnetic parameters to heavy metal concentration and PLI were evaluated with the software PAST (Hammer et al., 2001).

Individual particles were characterized with a JEOL JSM 6500F Field Emission (Schottky type) Scanning Electron Microscope (FE-SEM, resolution 1.5 nm at 15 kV operating voltage), equipped with backscattered electron detector and Energy Dispersion System (EDS, JEOL HYPERNINE, 133 eV resolution) microanalysis. Before FESEM observation, the samples were carbon-coated using a JEOL JEC-530 Auto Carbon Coater. The microscope working distance was 10 mm, with an accelerating voltage of 15 kV. EDS spectra were first acquired from randomly chosen particles to broadly characterize the PM, and subsequently from Fe-rich particles only, to investigate in detail the composition of the magnetic PM.

3. Results

3.1. Magnetic properties

3.1.1. Native lichens

The magnetic susceptibility values of the *Xanthoria parietina* native lichens, collected from both areas, range from 14.5 to 156.0×10^{-8} m^3/kg, always exceeding the value of the control lichen (10.8×10^{-8} m^3/kg) (Table 3, Fig. 3).

All the hysteresis loops, except for the sample S2 of the Via di Salone area, are similar in shape, saturated well before 1 T, with modest variability of the coercivity [11.3 mT < B_c < 13.7 mT; 35.6 mT < B_{cr} < 39.3 mT], indicating substantial uniformity of the magnetic mineralogy, presumably ascribable to magnetite or, in any case, soft ferrimagnetic minerals (Table 3, Fig. 4).

The sample S2 is anomalous, with the high saturation field (about 800 mT) not confirmed by the shape of the IRM acquisition (4m).

The variation of bulk magnetic susceptibility (k) vs temperature, performed on selected samples, confirmed that magnetite is the main magnetic mineral, being 580 °C the estimated Curie temperature (Fig. 5). The magnetothermic curves are noisy, possibly due to the burning of the organic matter, and the first, weak, inflection point at about 350 °C suggests the presence of maghemite. The decrease in magnetic susceptibility in the temperature range of 500 to 580 °C indicates either a wide grain-size distribution of magnetite or the presence of a mixture of magnetite and maghemite, in the form of a maghemitized rim on a magnetite core within the same magnetic particles, as it was studied for "technogenic" magnetic particles by Magiera et al., 2011.

Moreover, the decrease at 500 °C in some samples of cement dust, corresponding to two magnetic phases, appeared on the cooling curve of the cement samples observed by Magiera et al., 2013. The Hopkinson peak and a possible second order influence from titanomagnetite minerals, eventually arising from the substrate, could furtherly complicate the curves.

The magnetothermic curve of the sample S2 has the same inflection points observed for the other samples, and neither goethite nor hematite, as high saturation magnetic minerals, were observed through their estimated Curie/Néel temperatures.

In conformity with the magnetic susceptibility, the concentration dependent magnetic parameters vary by about one order of magnitude [$1.5 \times 10^{-2} < M_s$ (A m^2 kg^{-1}) $< 14.1 \times 10^{-2}$; $2.1 \times 10^{-3} < M_{rs}$ (A m^2 kg^1) $< 21.6 \times 10^{-3}$]. Overall, the hysteresis parameters indicate

Table 3
Magnetic susceptibility and hysteresis parameters, measured and computed for native and transplanted lichens.

Sample	χ (10^{-8} m^3/kg)	M_s (mAm^2/kg)	M_{rs} (mAm^2/kg)	B_c (mT)	B_{cr} (mT)	B_{cr}/B_c	M_{rs}/M_s
S0	37.0	53.0	7.6	12.9	39.0	3.03	0.14
S1	156.0	141.0	21.6	13.4	38.0	2.84	0.15
S2	55.1	113.0	9.3	11.7	36.8	3.13	0.82
S3	156	124.0	19.3	12.6	38.7	3.06	0.16
Valle Oracola (CO)	10.8	9.4	1.2	10.4	34.1	3.28	0.13
T1	40.6	62.4	8.9	12.4	37.6	3.04	0.14
T2	14.5	15.2	2.1	11.3	35.6	3.15	0.14
T3	22.6	22.5	3.1	11.7	37.7	3.22	0.14
T4	48.3	46.4	6.6	12.4	39.2	3.17	0.14
T5	85.4	99.4	14.1	13.0	39.4	3.04	0.14
TS1	9.7	4.5	0.7	12.4	38.7	3.13	0.16
TS2	17.1	12.1	1.8	13.0	39.7	3.06	0.15
TS3	8.7	3.8	0.6	13.3	39.7	2.98	0.17
TS4	9.2	9.0	1.2	12.0	40.8	3.39	0.14
TS5	7.4	5.7	0.8	11.9	36.9	3.09	0.15
TS7	7.1	7.0	1.0	11.6	37.6	3.24	0.14
Terminillo (CT)	3.4	0.8	0.2	15.4	47.7	3.09	0.28

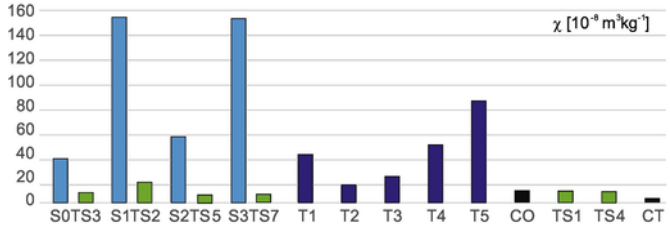

Fig. 3. Histograms of magnetic susceptibility χ: in light blue, native samples from via di Salone; in blue, native samples from Via Tiburtina; in green, transplants from via di Salone; in black, control samples; CO refers to the Valle Oracola control sample, CT to the Terminillo pre-exposure. Native and transplanted samples from the same sites are placed beside. (For interpretation of the references to colour in this figure legend, the reader is referred to the web version of this article.)

variable concentrations of very similar magnetic minerals; M_s and M_{rs} values are always higher than in the Valle Oracola control lichen ($M_s = 9.4 \times 10^{-3}\,A\,m^2\,kg^{-1}$; $M_{rs} = 1.2 \times 10^{-3}\,A\,m^2\,kg^{-1}$).

The M_{rs}/M_s vs B_{cr}/B_c ratios indicate that the samples are quite homogeneous and distributed in the central region of the Day Plot (Dunlop, 2002a, 2002b), attributable to prevailing Pseudo Single Domain (PSD) behavior (6), and in between the theoretical trends for SD-MD and SD-SP magnetite. Only the sample S2, already mentioned for the particular shape of the hysteresis loop, is relatively distant from the cluster formed by the other samples, placing in the proximity of the theoretical trend expected for a mix of 80% MD and 20% SD stoichiometric magnetite.

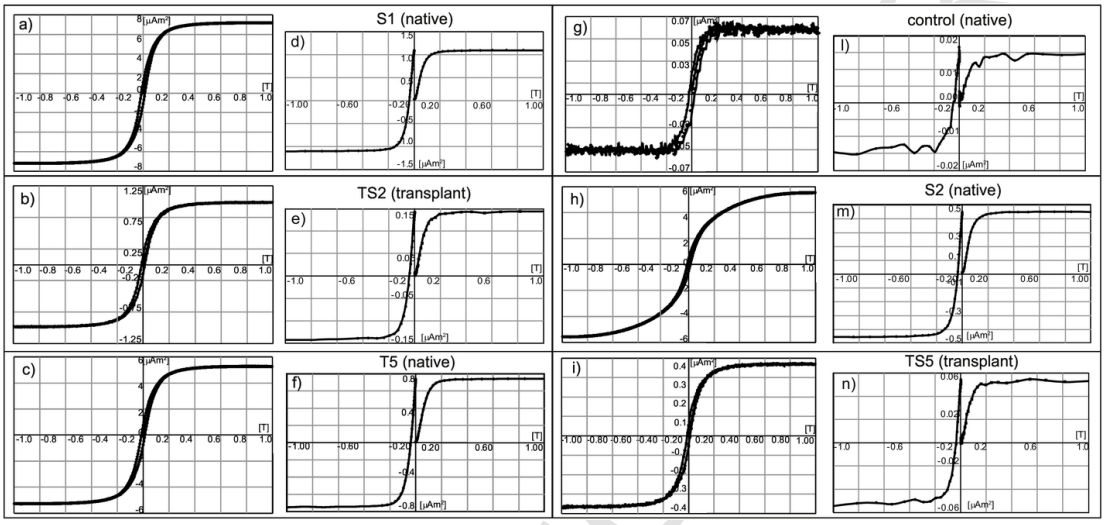

Fig. 4. Hysteresis loops and backfield application after saturation for selected specimens: a, d) S1 native sample, via di Salone; b, e) TS2 transplant, in the same site of S1; c, f) T5 native sample, from via Tiburtina; g, l) Valle Oracola control sample; h, m) S2 native sample; i, n) TS5 transplant, in the same site of S2. The second letter refers to isothermal remanent magnetization acquisition and back-field application curves. Hysteresis loops are corrected for the high field linear trend; values are not divided for the mass of the sample.

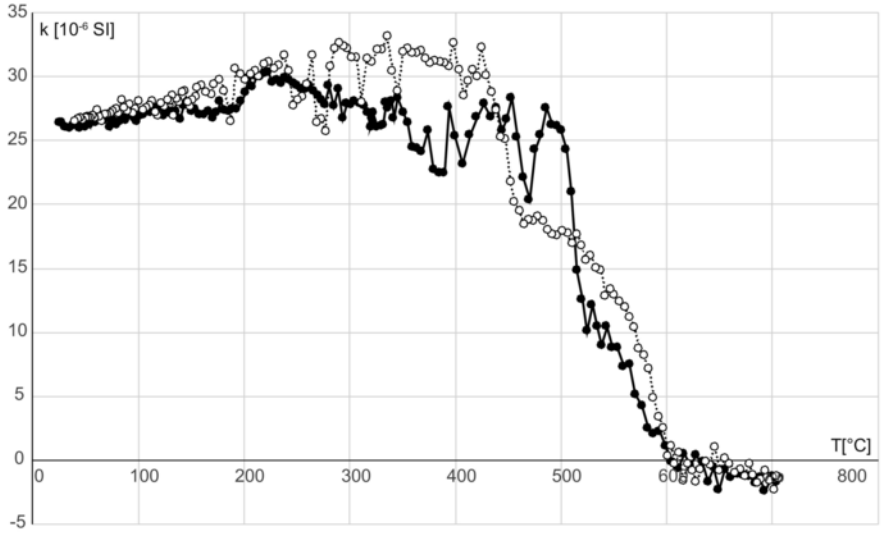

Fig. 5. Temperature variation of the magnetic susceptibility (k) for the native sample S3; black circles are for the heating process, open circles for the following cooling to room temperature. Data were corrected for the empty furnace. Heating and cooling cycles were performed in air.

3.1.2. Magnetic properties of the transplanted lichens

The values of the concentration dependent magnetic parameters are considerably lower in the transplanted lichens than in the native samples.

The magnetic susceptibility values of the *Pseudevernia furfuracea* transplants (Table 3, 3) range from 7.1×10^{-8} to $17.1\times10^{-8}\,m^3/kg^{-1}$, exceeding again the corresponding control lichen, whose magnetic susceptibility was the lowest of the set ($3.4\times10^{-8}\,m^3\,kg^{-1}$).

Despite the lower concentration of magnetic minerals, the hysteresis loops are well defined (Table 3, 4), and their parameters range from 3.8×10^{-3} to $12.1\times10^{-3}\,A\,m^2\,kg^{-1}$ for M_s and from 6.5×10^{-4} to $17.9\times10^{-4}\,A\,m^2kg^{-1}$ for M_{rs}; B_c ranges from 11.6 to 13.3 mT and B_{cr} and from 36.9 to 40.8 mT, overlapping the coercivity values of the *Xanthoria parietina* native samples.

Sample TS2, from the entrance wall of the dismissed cement plant, stands out for the values of the concentration dependent magnetic parameters.

Also for transplants, the values of the concentration dependent magnetic parameters are higher than the pre-exposure sample.

In the Day plot (Fig. 6), the magnetic grain size was homogeneous to that of the native samples, indicating, again, the prevalence of PSD domain state.

FORC diagrams of native and transplanted samples S1 and TS2, from the same site in via di Salone, and Terminillo pre-exposure are shown in Fig. 7; S1 and TS2 show prevailing pseudo single domain (PSD) features, even if the discrimination between PSD and a mixture of single domain (SD) and multidomain (MD) is not straightforward with these kind of diagrams (Roberts et al., 2000).

The FORC diagram of S1 also indicates a slightly higher coercivity range, with the occurrence of low interaction SD features (Fig. 7c).

Overall, low-coercivity characteristics prevail in all the samples, including the pre-exposure Terminillo sample.

The presence of ultrafine superparamagnetic (SP) magnetic particles was negligible; it was estimated measuring the 100 s decay of remanent magnetization after the application of a saturation magnetic field, which is indicative of the remanence fraction carried by particles in the SP-SD boundary (Wang et al., 2010; Sagnotti and Winkler, 2012).

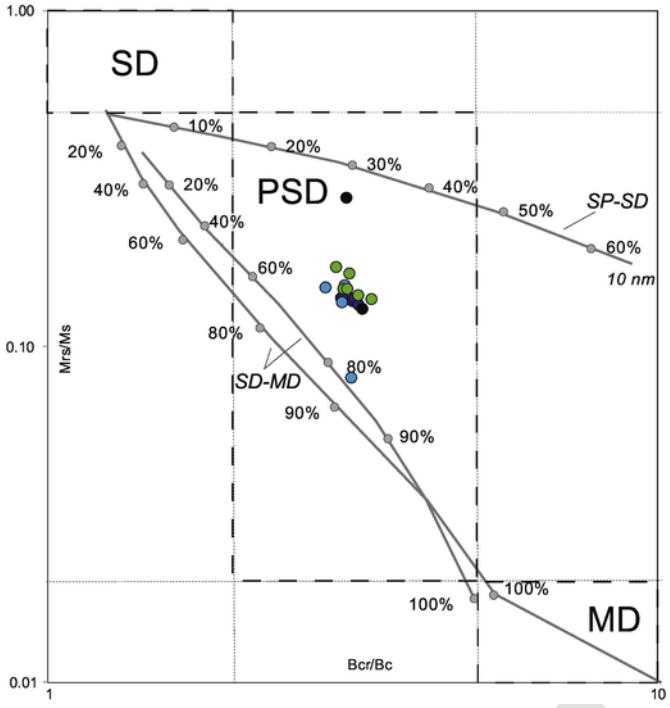

Fig. 6. Logarithmic Day plot of the hysteresis ratios M_{rs}/M_s vs. B_{cr}/B_c for native lichens from via di Salone (light-blue) and from Tiburtina (blue), for transplants from via di Salone (green) and for control samples (black). The SD (single domain), PSD (pseudo-single domain) and MD (multidomain) fields and the theoretical mixing trends for SD-MD and SP-SD grains (SP, superparamagnetic) are from Dunlop (2002a, 2002b) and refer to magnetite. (For interpretation of the references to colour in this figure legend, the reader is referred to the web version of this article.)

3.2. Chemical analyses

The concentration of heavy metals, including the normalization to the control/pre-exposure concentration and the Tomlinson PLI pollution index, are reported in Tables 4 and 5, for native and transplanted samples, respectively.

The element concentrations of *Xanthoria parietina* sampled near Vvia di Salone and in Via Tiburtina can be visualized, in Table 6 through the chromatic scale proposed in Cecconi et al., 2019, referring to the background elemental content (BEC), and updating previous works by Nimis and Bargagli, 1999 and Nimis et al., 2000. In Cecconi et al., 2019, Fe and Mn were excluded from the analyses of native samples. In the study area, the most of the elements are rated as High and Severe bioaccumulation levels.

For transplants, the same method has been used according to the classes introduced in Cecconi et al., 2019, but referring, for this study, to the metals concentration of the pre-exposure sample (Table 7); thus, using the exposed-to-control (EC) ratio, instead of the exposed-to-unexposed (EU) ratio therein suggested, in order to classify also Fe and Mn.

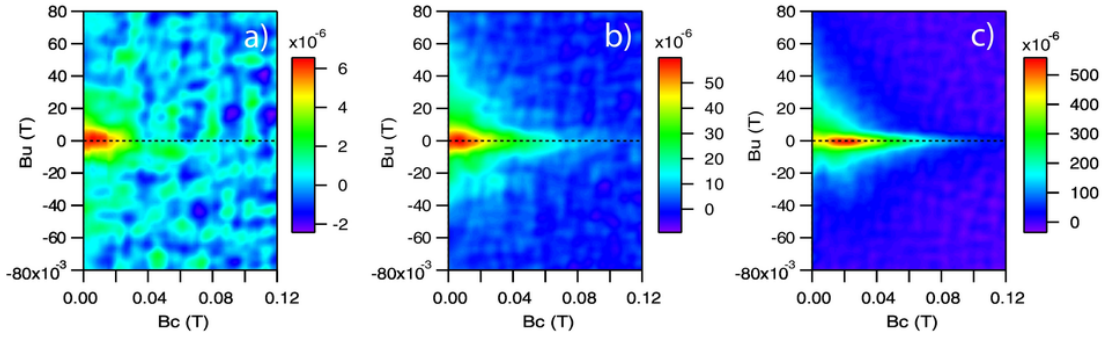

Fig. 7. FORC (First Order Reversal Curve) diagrams for a) pre-exposure sample, b) transplant TS2 (b) and c) native S1; the smoothing factor was, respectively, 10, 7 and 4.

Table 4
Concentration (mg/kg), normalization to the control sample and PLI of heavy metals in native *Xanthoria parietina* samples.

	Hg Hg/Hg_{cont}	As As/As_{cont}	Cr Cr/Cr_{cont}	Cu Cu/Cu_{min}	Ni Ni/Ni_{cont}	Cd Cd/Cd_{cont}	Pb Pb/Pb_{cont}	Mn Mn/Mn_{cont}	Fe Fe/Fe_{cont}	Zn Zn/Zn_{cont}	PLI
S0	4.30	26.00		29.00	15.00	0.13	22.00	50.0	3241	41	3.32
	430.0	51.0		3.6	5.3	0.7	3.7	3.4	1.4	1.3	
S1	0.06	18.67	16.03	32.46	10.00	0.23	49.39	287.0	9772	106	5.57
	6.0	36.6	3.6	4.0	3.5	1.2	8.4	19.7	4.3	3.4	
S2	0.26	2.96	5.73	22.05	4.00	0.09	8.97	61.0	2916	43	1.74
	26.0	5.8	1.3	2.7	1.4	0.5	1.5	4.2	1.3	1.4	
S3	0.15	3.97	19.64	65.11	8.03	0.12	23.2	158.0	5908	106	3.83
	15.0	7.8	4.5	8.0	2.8	0.6	4.0	10.8	2.6	3.4	
T1	0.11	1.50	4.09	17.62	2.62	0.14	4.42	58.0	3306	82	1.52
	11.0	2.9	0.9	2.2	0.9	0.7	0.8	4.0	1.4	2.7	
T2	0.20	1.01	3.01	11.46	8.66	0.15	2.58	38.0	2068	70	1.29
	20.0	2.0	0.7	1.4	3.1	0.8	0.4	2.6	0.9	2.3	
T3	0.40	1.23	4.71	12.45	2.51	0.20	5.31	49.0	2063	36	1.31
	40.0	2.4	1.1	1.5	0.9	1.0	0.9	3.4	0.9	1.2	
T4	0.27	3.45	7.68	32.78	5.13	0.09	12.66	101.6	4720	50	2.32
	27.0	6.8	1.8	4.0	1.8	0.5	2.2	7.0	2.1	1.6	
T5	6.11	2.56	6.24	19.90	2.37	0.33	8.53	58.0	3737	47	1.91
	611.0	5.0	1.4	2.4	0.8	1.7	1.5	4.0	1.6	1.5	
Control Valle Oracola (CO)	0.01	0.51	4.40	8.16	2.84	0.20	5.88	14.6	2287	31	1.00
	1.0	1.0	1.0	1.0	1.2	2.2	2.3	1.0	1.1	1.0	

Table 5
Concentration (mg/kg), normalization to the pre-exposure sample and PLI values of heavy metals in transplanted Pseudevernia furfuracea samples.

	As As/As_{pre}	Cr Cr/Cr_{pre}	Cu Cu/Cu_{pre}	Ni Ni/Ni_{pre}	Cd Cd/Cd_{pre}	Pb Pb/Pb_{pre}	Mn Mn/Mn_{pre}	Fe Fe/Fe_{pre}	Zn Zn/Zn_{pre}	PLI
TS1	0.29	4.52	25.00	2.62	0.28	5.30	36.6	258	18.3	1.83
	1.9	1.7	3.8	1.4	1.1	4.9	1.9	1.2	1.1	
TS2	0.43	6.69	17.27	7.45	0.22	12.69	38.1	1182	36.5	2.97
	2.9	2.5	2.6	4.0	0.9	11.6	2.0	5.5	2.1	
TS3	0.38	4.08	16.68	2.44	0.27	7.88	27.3	525	21.9	1.97
	2.5	1.5	2.5	1.3	1.1	7.2	1.4	2.5	1.3	
TS4	0.40	3.49	17.84	2.2	0.25	5.38	34.3	319	25.4	1.82
	2.7	1.3	2.7	1.2	1.0	4.9	1.8	1.5	1.5	
TS5	0.50	4.24	17.39	3.1	0.28	13.48	34.6	598	41.7	2.52
	3.3	1.57	2.6	1.7	1.1	12.4	1.8	2.8	2.4	
TS7	0.43	3.12	16.22	2.19	0.24	9.91	40.7	695	34.3	2.19
	2.9	1.2	2.5	1.2	1.0	9.1	2.1	3.3	2.0	
Pre-exposure Terminillo (CT)	0.15	2.70	6.59	1.84	0.25	1.09	19.2	213	17.1	1.00
	1.0	1.0	1.0	1.0	1.0	1.0	1.0	1.0	1.0	

Table 6
Analytical results on *Xanthoria parietina*; colour scale according to Cecconi et al., 2019 and referred to the background elemental content (BEC).

	Hg	As	Cr	Cu	Ni	Cd	Pb	Zn
S0	122.9	173.3		6.4	9.1	1.9	22.0	1.9
S1	1.7	124.5	10.0	7.2	6.1	3.3	49.4	5.0
S2	7.4	19.7	3.6	4.9	2.4	1.3	9.0	2.0
S3	4.3	26.5	12.2	14.5	4.9	1.7	23.2	5.0
T1	3.1	10.0	2.5	3.9	1.6	2.0	4.4	3.8
T2	5.7	6.7	1.9	2.5	5.3	2.1	2.6	3.3
T3	11.4	8.2	2.9	2.8	1.5	2.9	5.3	1.7
T4	7.7	23.0	4.8	7.3	3.1	1.3	12.7	2.3
T5	174.6	17.1	3.9	4.4	1.4	4.7	8.5	2.2

Absence of bioaccumulation	Low bioaccumulation	Moderate bioaccumulation	High bioaccumulation	Severe bioaccumulation

Table 7
Analytical on *Pseudevernia furfuracea*; the colour scale according to Cecconi et al., 2019 is referred to exposed-to-control (EC) ratio.

	As	Cr	Cu	Ni	Cd	Pb	Mn	Fe	Zn
TS1	1.9	1.7	3.8	1.4	1.1	4.9	1.9	1.2	1.1
TS2	2.9	2.5	2.6	4.0	0.9	11.6	2.0	5.5	2.1
TS3	2.5	1.5	2.5	1.3	1.1	7.2	1.4	2.5	1.3
TS4	2.7	1.3	2.7	1.2	1.0	4.9	1.8	1.5	1.5
TS5	3.3	1.6	2.6	1.7	1.1	12.4	1.8	2.8	2.4
TS7	2.9	1.2	2.5	1.2	1.0	9.1	2.1	3.3	2.0

Absence of bioaccumulation	Low bioaccumulation	Moderate bioaccumulation	High bioaccumulation	Severe bioaccumulation

3.3. Morphoscopic observations

The morphological observations mostly pointed out iron-rich round shaped particles, fully incorporated into the lichens tissues (Fig. 8a), usually in the dimensional range from 1 to 10 μm, occasionally with rough and bright surfaces or given by the aggregation of different submicrometric particles (Fig. 8b).

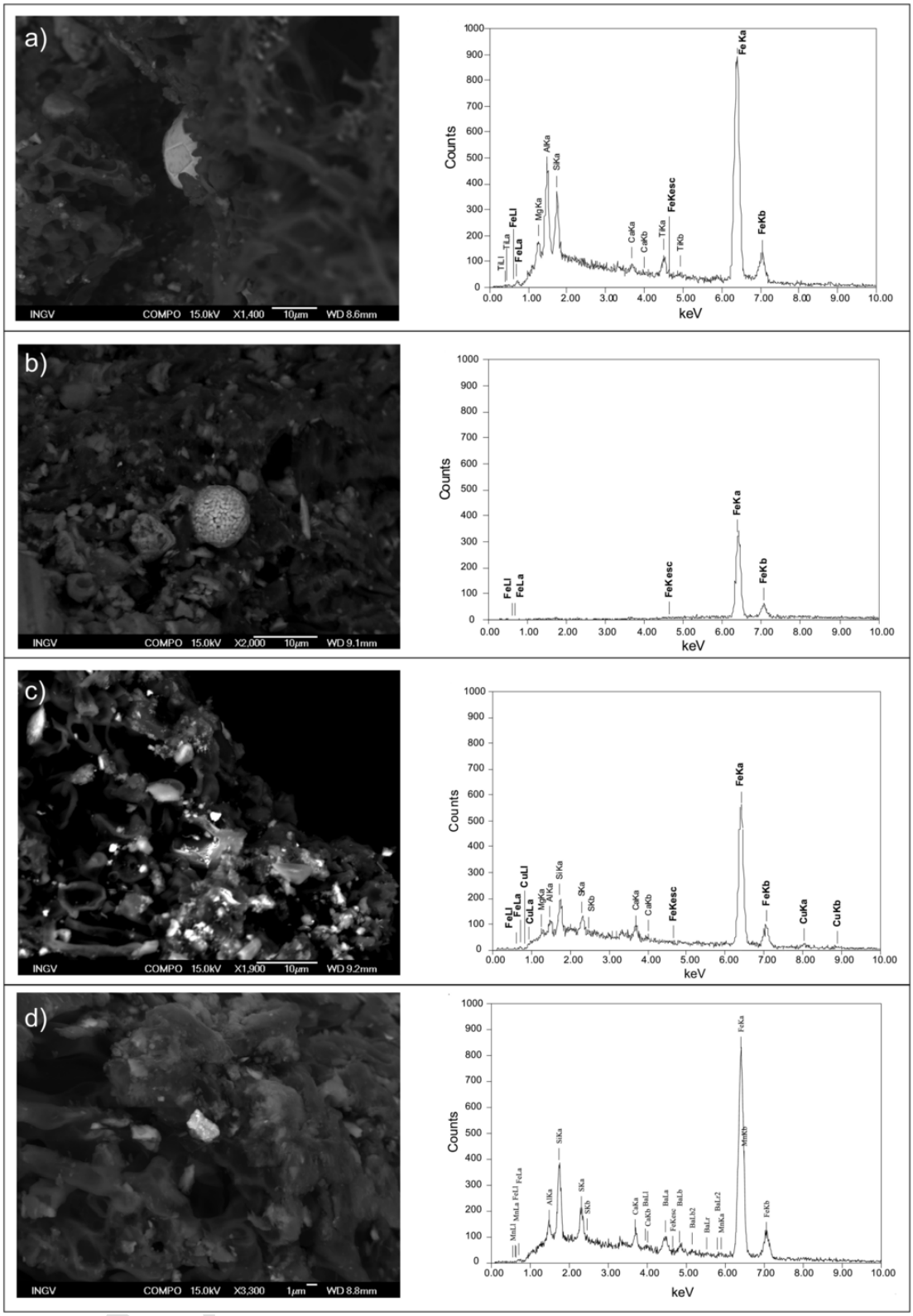

Fig. 8. FESEM images and EDS spectra of selected particles embedded in the lichens from via di Salone; (a) spherical iron-rich particle; (b) iron–rich spherical aggregate; (c) iron-rich, with Cu inclusions, micrometric particles (d) iron-rich, with Ba inclusions, irregularly shaped grain.

The chemical composition of selected particles, characterized through EDS X-ray microanalysis, indicated that other metals, as Mn, Cu (Fig. 8c), Cr and Ba (Fig. 8d), are widely present under different proportions.

4. Discussion

4.1. Magnetic properties and morphoscopic features of the lichens

The magnetic susceptibility χ values measured in native samples, ranging from 14.5 to $156.0 \times 10^{-8}\,m^3/kg$, are indicative of considerable concentrations of magnetic minerals. This result is compatible with the recent review by Hofman et al., 2017, where the values of susceptibility for mosses and lichens are distributed between −1.5 and $+1161.0 \times 10^{-8}\,m^3/kg$ (the latter relative to metallurgy zones near Tandil, Argentina on lichen *Parmotrema pilosum*; Marié et al., 2016).

The χ values from via di Salone and via Tiburtuna areas are higher than those obtained from *Xanthoria parietina* native lichens sampled near a cement plant in Slovakia, which showed magnetic susceptibility values ranging from 7 to $92 \times 10^{-8}\,m^3/kg$ (Paoli et al., 2017).

The χ values are also noticeable higher if compared to magnetic biomonitoring studies on *Quercus ilex* and *Platanus* leaves from a southeastern quadrant of Rome (Moreno et al., 2003; Szönyi et al., 2007; Szönyi et al., 2008), even considering the different characteristics of deposition and accumulation of PM on leaves.

In the study area, it was possible to find only a few lichens; for this reason, lichen transplants were placed around the same sites where native samples were taken; after four months of exposure, the values of the concentration dependent magnetic parameters doubled, at least, those from the pre-exposure sample, even if they were considerably lower than those from the native samples.

Noteworthy, the magnetic susceptibility value of the pre-exposure sample from Terminillo was about one order of magnitude higher with respect to those considered in Kodnik et al., 2017, which were collected in a pristine area of the Carnic Alps, probably for the influence of a different bedrock, but also for roads and houses nearby to the small wood. Thus, it is advisable to perform pre-exposure analyses before transplanting the lichens.

Previous studies have already highlighted, for transplants, noticeably lower values of magnetic susceptibility with respect to the native samples, as observed for lichens *Evernia prunastri* exposed for six months near a Slovak cement factory (Paoli et al., 2017). In Kodnik et al., 2017, *Pseudevernia furfuracea* lichen transplants exposed for two months in an industrial area in the province of Pordenone showed magnetic susceptibility values ranging from 0.35 to $7.41 \times 10^{-8}\,m^3/kg$. Thus, relatively to previous studies involving transplant, it is possible to confirm that the magnetic properties reflect a relevant bioaccumulation of magnetic particles in the study area.

As summarized in Cecconi et al., 2019, transplanted lichens are usually exposed for few weeks to harsh environmental conditions; thus they bio-accumulate mostly through passive mechanisms (Nieboer et al., 1978, Nash III, 2008). By contrast, the bioaccumulation in lifespan-exposed native lichens, even decades, is the result of a long-term interaction between passive phenomena and slower active intracellular uptakes characterized by element-specific kinetics (Brown and Beckett, 1984), achieving a dynamic equilibrium with the surrounding environment, with higher elemental concentration levels in the case of important pollutant loads (Paoli et al., 2018).

The Day Plot (Fig. 6) highlights that the magnetic mineralogy of the lichens is almost uniform, corresponding to magnetite-like minerals in PSD magnetic domain state/grain size, roughly corresponding to particle size ranging between 0.1 μm and 15 μm, considering that the critical magnetic grain size transitions, theoretically determined for equidimensional magnetite, are about 0.03 μm for SP to SD, 0.08 μm for SD to PSD, 17 μm for PSD to true MD (Butler and Banerjee, 1975). Noteworthy, data fall in the central-upper part of the PSD region, likewise the diesel exhaust emissions in Sagnotti et al., 2009, and far from the lower right corner of plot, where, usually, dusts from brakes fall. The general magnetic behavior seems more connected to combustion dusts, than to coarser traffic related abrasion grains.

FORC diagrams (Fig. 7) generally confirm what was pointed out by the Day Plot and indicate the progressive accumulation of magnetic particles in the post-exposure samples, as suggested by the noisy diagram and the high smoothing factor of the pre-exposure sample, moving towards well defined - low smoothing factor diagrams for the native samples. FORC diagrams confirm that pre-transplant samples originally had lower but well recognizable magnetic properties, probably connected to the anthropic sources around. SD features emerge in the diagram from the native sample, possibly for the more accurate elaboration due to the higher magnetic minerals content.

In general, the use of FORC diagrams demonstrates that SD particles, also in environmental magnetism studies, are more common than was previously recognized through the Day diagram only, considering that a wide range of factors, such as mixing with SP, PSD, or MD particles and thermal relaxation biases against recognition of SD behavior when using the Day plot (Roberts et al., 2018).

There is no relevant presence of ultrafine magnetic particles in SP state – enhancing the magnetic susceptibility values – looking at Day plot, FORC diagrams and remanent magnetization decay. Moreover, in traffic-related PM, the SP fraction mainly occurs as coating of MD particles and is originated by localized stress in the oxidized outer shell surrounding the unoxidized core of magnetite-like grains, and cannot be considered as a direct proxy for the overall content of ultrafine particles (Sagnotti and Winkler, 2012).

Taking in account the different bioaccumulation mechanisms of native and transplanted lichens, the overall homogeneity of data confirms the hypothesis that the magnetic parameters are mainly linked to the same anthropogenic sources of PM, independently of the location, the exposure and the lichen species. The only sample with slightly different magnetic properties was S2, taken from a low tree facing a canal bringing wastewater to Aniene river; the corresponding transplant, TS5, was quite homogenous to the rest of the set. Perhaps, the hysteresis loop of sample S2 was influenced by the presence of high saturation field magnetic minerals, maybe from natural sources or soils. By contrast, coercivities, saturation of the isothermal remanent magnetization, backfield application, magnetothermic curves and FORC diagram do not support this hypothesis.

The grain-size of these particles has been confirmed by the morphoscopic observations of round shaped particles, fully incorporated into the lichens tissues, usually ranging from 1 to 10 μm, although submicrometric particles may be too small to be seen at SEM.

Their chemical composition, carried out by EDS X-ray microanalysis, highlighted the presence of elements as Cr, Mn, Cu and Ba, the latter usually connected to emissions from car brakes and tyres, as observed by Sanders et al. (2003) and Sagnotti et al. (2009), as well as metallic residuals arising from plenty of anthropic sources. The shape and the recurrent inclusion of various elements other than Fe in these magnetic particles make them different from natural stoichiometric magnetite grains. Many observed morphologies are similar to the spherical shapes of industrial fly ashes originated by combustion of black and brown coal (e.g., Sarbak et al., 2004; Veneva et al.,

2004; Jordanova et al., 2004, 2006), deriving from a combustion source and different to traffic related dusts from brakes emissions (Sagnotti et al., 2009).

4.2. Linear correlation between magnetic properties and elemental concentration

In order to verify that χ is representative of the same magnetic fraction carried by other concentration-dependent magnetic parameters, its values were correlated to M_s and M_{rs} values from hysteresis loops. In native samples, these parameters were linearly correlated at a 99% confidence level (p-value < 0.01), and better than 95% for the transplants (Table 8). This correlation further improves neglecting the sample S2, which was previously discussed for its peculiar hysteresis loop and the position in the Day Plot. These results highlight that χ, M_s and M_{rs} are indicative of the same magnetic fraction and that magnetic susceptibility is confirmed a good proxy for the concentration of the ferromagnetic fraction of PM.

Since magnetic susceptibility is the most rapid and sensitive magnetic parameter to be measured, its values were considered for evaluating its linear correlation with the metals concentration and PLI.

According to the *p_value*, the hypothesis that magnetic susceptibility is linearly correlated to elemental concentration cannot be rejected at 99% confidence level, for the full set of samples, for Cr, Cu, Pb, Mn, Fe and Zn. For transplants only, there is a general decrease in the quality of the linear regressions, and only Cr, Ni and Fe are linearly correlated to χ, at 95% confidence level (Table 8).

In this case, it must be taken into account that the values of magnetic susceptibility are at the sensitivity limits of the instrument, and that the metals concentration are low, thus affecting the quality of the results and the reliability of these correlations. Moreover, the low values of magnetic susceptibility are probably slightly underestimated and affected by the diamagnetism of the lichens, which is overcome by the ferromagnetic fraction only when its abundance is relevant.

Overall, considering the statistics on the full set, independently of the lichen species and of the exposure duration, the concentration dependent magnetic parameters resulted significantly correlated to the abundance of Cr, Fe, Cu, Pb, Mn, and Zn, which appear to be the main elements connected to the anthropic activities on this area.

The linear correlations of χ with PLI are significant at 99% for transplants, native samples and for the whole set.

Table 8
*p*_values of the linear correlation between magnetic susceptibility, element concentration and PLI in native and transplanted lichens; in bold the values which are significant at 99% level of confidence; on parenthesis, only for the full set, the coefficient of linear determination.

Magnetic parameter (*), element	*p*_value χ vs concentration and PLI, full set, confidence level 99%, r^2	*p*_value χ vs concentration and PLI, native only, confidence level 99%	*p*_value χ vs concentration and PLI, transplants only, confidence level 95%
M_s*	**<0.01** (r^2=0.86)	**<0.01**	**<0.05**
M_{rs}*	**<0.01** (r^2=0.96)	**<0.01**	**<0.05**
Hg	0.97 (r^2=0.00)	0.97	
As	0.06 (r^2=0.21)	0.40	0.29
Cr	**<0.01** (r^2=0.84)	**<0.01**	**<0.05**
Cu	**<0.01** (r^2=0.61)	**<0.01**	0.26
Ni	0.09 (r^2=0.18)	0.47	**<0.05**
Cd	0.36 (r^2=0.06)	0.63	0.30
Pb	**<0.01** (r^2=0.59)	**<0.01**	0.20
Mn	**<0.01** (r^2=0.79)	**<0.01**	0.18
Fe	**<0.01** (r^2=0.83)	**<0.01**	**<0.05**
Zn	**<0.01** (r^2=0.70)	**<0.01**	0.41
PLI	**<0.01** (r^2=0.56)	**<0.01**	**<0.05**

The elements Cd and Hg reported the worst correlations with χ; Cd was the less bioaccumulated according to Tables 6 and 7, while Hg unusual values, especially for samples S0 and T5, are probably outliers.

Moreover, the decreased levels of bioaccumulated elements for the transplants (Table 7), with respect to the native samples (Tab. 6), and in agreement with the magnetic measurements, may be due to the heavy rainfalls in the last period of exposure and to the relevant elemental concentration of the pre-transplant sample, as previously discussed, probably biasing the EC ratios.

Anyway, these considerations are mostly qualitative, due to the intrinsic limits in the definition of the EC ratio; recently, a method based on the calculation of EC ratios of element concentrations and on the quantification of the associated uncertainty has been suggested, to allowed the selection of significantly accumulated elements, as well as the evaluation whether a site is significantly polluted or not (Loppi et al., 2019).

The accumulation of metals was evident in the investigated samples, even with the limitations due to the complexity of the investigated area, mainly for the presence of many sources of pollution, among which combustion events that involved both natural and anthropic material (fossil fuels, plastics, materials containing flame-retardants and metals).

The Roma camp, where arsons are set, is located in a heavily populated area where, in addition to outdoor combustion, there are road infrastructures, building sites and industrial and craft activities. It was therefore not possible to determine and discriminate the influence of such various anthropogenic sources in the production, diffusion and accumulation of airborne micropollutants. Cu, which is the main element involved in fraudulent fires, is also widely used in automotive industry; the motor industry uses copper for mechanical, electrical and electronic installations, so that it is estimated that each vehicle contains, at least 18 kg of copper (Lipowsky and Arpaci, 2007).

Bioaccumulation was well represented by the magnetic properties, even if, due to the scarce presence of lichens, it was not possible to identify the distribution patterns of the PM and to understand the reasons of the relatively high variations (about one order of magnitude) of the concentration dependent magnetic parameters and, accordingly, of the metal concentrations. Anyway, the multidisciplinary approach and the good matching of the results possibly overcome this aspect, also considering that the most of the PM observations are usually carried out from single monitoring stations covering definitely larger areas.

5. Conclusions

This pilot study was carried out to stimulate the multidisciplinary analysis of airborne particulate matter near sites affected by fraudulent fires and other anthropogenic polluting sources. The set of samples, even if small and distributed in a complex area, was magnetically uniform and inspires further research on the magnetic particles and parameters arising from heterogeneous anthropic sources. Schematically, the main results that emerged are:

1) The magnetic mineralogy of native and transplanted lichens from two different sites in the easternmost side of Rome, Italy, was almost uniform and mostly corresponds to combustion related magnetite-like minerals in pseudo single domain magnetic state. The grain-size - crossing magnetic and SEM observations - mostly ranges from submicrometric to 10 μm.
2) The homogeneity of the parameters related to the magnetic mineralogy and grain-size favor the hypothesis that they are linked to

the same anthropogenic sources of PM, independently of the location, the exposure time and of lichen species.

3) The values of the concentration dependent magnetic parameters and the results of their linear regressions with the element concentration indicate that the relevant concentrations of magnetic minerals are connected to the abundance of Fe, Cr, Pb, Mn, Zn and Cu.
4) FESEM observations showed the relevant presence of Fe-rich spherules, in the same grain-size range determined with the magnetic properties, with recurrent inclusion of Mn, Cu and Cr. The morphologies were mostly similar to spherical shapes arising from combustion.

Overall, magnetic properties and, in particular, magnetic susceptibility, are valid proxies of airborne particulate matter, even in a complex area, where many different sources of pollution are present and their discrimination is not fully feasible.

Further developments need to be carried out thickening the survey grid and repeating the observations in different periods of the year, focusing on the discrimination of the anthropic emissions through the observation of single-source areas, in order to focalize their different roles in the overall pollution load due to airborne particulate matter.

Supplementary data to this article can be found online at https://doi.org/10.1016/j.scitotenv.2019.06.526.

Uncited reference

Tomlinson et al., 1980

Acknowledgements

Part of this research (magnetic analyses) was funded and included in the framework of FISR2016 project, promoted by MIUR, the Italian Ministry of Education, University and Research. The authors are grateful to the reviewers for their in-depth revisions, which substantially improved the manuscript, and to the Associate Editor, Elena Paoletti, for carefully managing the revision. AW is grateful to Stefano Loppi for introducing him to lichen biomonitoring and for the fruitful suggestions and discussions.

References

Adamo, P., Crisafulli, P., Giordano, S., Minganti, V., Modenesi, F., Monaci, P., Pittao, E., Tretiach, M., Bargagli, C., 2007. Lichen and moss bags as monitoring device in urban areas, part II: trace elements content in living and dead biomonitors and comparison with synthetic materials. Environ. Pollut. 146, 392–399.

Adamo, P., Bargagli, R., Giordano, S., Modenesi, P., Monaci, F., Pittao, E., Spagnuolo, V., Tretiach, M., 2008. Natural and pre-treatments induced variability in the chemical composition and morphology of lichens and mosses selected for active monitoring of airborne elements. Environ. Pollut. 152, 11–19.

Augusto, S., Máguas, C., Branquinho, C., 2013. Guidelines for biomonitoring persistent organic pollutants (POPs), using lichens and aquatic mosses – a review. Environ. Pollut. 180, 330–338.

Augusto, S., Pinho, P., Santosa, A., Botelhoc, M.J., Palma-Oliveirac, J., Branquinho, C., 2015. Declining trends of PCDD/Fs in lichens over a decade in a Mediterranean area with multiple pollution sources. Sci. Total Environ. 508, 95–100.

Bargagli, R., Mikhailova, I., 2002. Accumulation of inorganic contaminants. In: Nimis, P.L., Scheidegger, C., Wolseley, P.A. (Eds.), Monitoring with Lichens – Monitoring Lichens. Kluwer Academic Publ, Amsterdam, pp. 65–84.

Bargagli, R., Nimis, P.L., 2002. Guidelines for the use of epiphytic lichens as biomonitors of atmospheric deposition of trace metals. In: Nimis, P.L., Scheidegger, C., Wolseley, P.A. (Eds.), Monitoring with Lichens - Monitoring Lichens. Kluwer Acad. Publ, Amsterdam, pp. 295–299.

Bari, A., Rosso, A., Minciardi, M.R., Troiani, F., Piervittori, R., 2001. Analysis of heavy metals in atmospheric particulates in relation to their bioaccumulation in explanted Pseudevernia furfuracea thalli. Environ. Monit. Assess. 69, 205–220.

Böhm, P., Wolterbeek, H., Verburg, T., Mulisek, L., 1998. The use of tree bark for environmental pollution monitoring in the Czech Republic. Environ. Pollut. 102, 243–250.

Branquinho, C., Gaio-Oliveira, G., Augusto, S., Pinho, P., Máguas, C., Correia, O., 2008. Biomonitoring spatial and temporal impact of atmospheric dust from a cement industry. Environ. Pollut. 151, 292–299.

Brown, D.H., Beckett, R.P., 1984. Uptake and effect of cations on lichen metabolism. Lichenologist 16, 173–188.

Brunialti, G., Frati, L., 2014. Bioaccumulation with lichens: the Italian experience. Int. J. Environ. Stud. 71, 15–26.

Cecconi, E., Fortuna, L., Benesperi, R., Bianchi, E., Brunialti, G., Contardo, T., Di Nuzzo, L., Frati, L., Monaci, F., Munzi, S., et al., 2019. New interpretative scales for lichen bioaccumulation data: the Italian proposal. Atmosphere 10, 136.

Chaparro, M.A., Lavornia, J.M., Chaparro, M.A., Sinito, A.M., 2013. Biomonitors of urban air pollution: magnetic studies and SEM observations of corticolous foliose and microfoliose lichens and their suitability for magnetic monitoring. Environ. Pollut. 172, 61–69.

Day, R., Fuller, M., Schmidt, V.A., 1977. Hysteresis properties of titanomagnetites: grain-size and compositional dependence. Phys. Earth Planet. Inter. 13, 260–267.

Dunlop, D.J., 2002. Theory and application of the Day plot (M_{RS}/M_S versus H_{CR}/H_C) 1. Theoretical curves and tests using titanomagnetite data. J. Geophys. Res. 107, https://doi.org/10.1029/2001JB000486.

Dunlop, D.J., 2002. Theory and application of the Day plot (M_{RS}/M_S versus H_{CR}/H_C) 2. Application to data for rocks, sediments, and soils. J. Geophys. Res. 107, https://doi.org/10.1029/2001JB000487.

Fabian, K., Reimann, C., McEnroe, S.A., Willemoes-Wissing, B., 2011. Magnetic properties of terrestrial moss (Hylocomium splendens) along a north-south profile crossing the city of Oslo, Norway. Sci. Total Environ. 409, 2252–2260.

Flanders, P.J., 1994. Collection, measurement, and analysis of airborne magnetic particulates from pollution in the environment. J. Appl. Phys. 75, 5931–5936.

Frati, L., Brunialti, G., Loppi, S., 2005. Problems related to lichen transplants to monitor trace element deposition in repeated surveys: a case study from central Italy. J. Atmos. Chem. 52, 221–230.

Gallo, L., Corapi, A., Loppi, S., Lucadamo, L., 2014. Element concentrations in the lichen Pseudevernia furfuracea (L.) Zopf transplanted around a cement factory (S Italy). Ecol. Indic. 46, 566–574.

Georgeaud, V.M., Rochette, P., Ambrosi, J.P., Vandamme, D., Williamson, D., 1997. Relationship between heavy metals and magnetic properties in a large polluted catchment: the Etang de Berre (south of France). Phys. Chem. Earth 22, 211–214.

Guidotti, M., Lucarelli, E., Onorati, B., Ravaioli, G., De Simone, C., Owczarek, M., 2000. Traffic pollution monitoring using mosses as bioaccumulator of metals and PAH. Ann. Chim. 90, 145–151.

Guidotti, M., Stella, D., De Marco, A., Owczarek, M., De Sinone, C., 2003. Lichens as PAHs bioaccumultors used in atmospheric pollution studies. Jour. Chrom. A 985 (1–2), 185–190.

Guidotti, M., Stella, D., Dominici, C., Blasi, G., Owczarek, M., Vitali, M., Protano, C., 2009. Monitoring of traffic-related pollution in a province of Central Italy with transplanted lichen Pseudovenia furfuracea. Bull. Environ. Contam. Toxicol. 83, 852–858.

Hammer, , Harper, D.A.T., Ryan, P.D., 2001. PAST: paleontological statistics software package for education and data analysis. Palaeontol. Electron. 4 (1), 9.

Hansard, R., Maher, B.A., Kinnersley, R., 2011. Biomagnetic monitoring of industry-derived particulate pollution. Environ. Pollut. 159, 1673–1681.

Hansard, R., Maher, B.A., Kinnersley, R.P., 2012. Rapid magnetic biomonitoring and differentiation of atmospheric particulate pollutants at the roadside and around two major industrial sites in the U.K. Environ. Sci. Technol. 46 (8), 4403–4410. https://doi.org/10.1021/es203275r.

Hofman, J., Maher, B.A., Muxworthy, A.R., Wuyts, K., Castanheiro, A., Samson, R., 2017. Biomagnetic monitoring of atmospheric pollution: a review of magnetic signatures from biological sensors. Environ Sci Technol 51 (12), 6648–6664.

Hunt, A., Jones, J., Oldfield, F., 1984. Magnetic measurements and heavy metals in atmospheric particles of anthropogenic origin. Sci. Total Environ. 33, 129–139.

Jordanova, D., Hoffmann, V., Fehr, K.T., 2004. Mineral magnetic characterization of anthropogenic magnetic phases in the Danube river sediments (Bulgarian parts). Earth Planet. Sci. Lett. 221, 71–89. https://doi.org/10.1016/S0012-821X(04)00074-3.

Jordanova, D., Jordanova, N., Hoffmann, V., 2006. Magnetic mineralogy and grain-size dependence of hysteresis parameters of single spherules from industrial waste products. Phys. Earth Planet. Inter. 154, 255–265. https://doi.org/10.1016/j.pepi.2005.06.015.

Jordanova, D., Petrov, P., Hoffmann, V., Gocht, T., Panaiotu, C., Tsacheva, T., Jordanova, N., 2010. Magnetic signature of different vegetation species in polluted environment. Stud. Geophys. Geod. 54, 417–442.

Kodnik, D., Candotto Carniel, F., Licen, S., Tolloi, A., Barbieri, P., Tretiach, M., 2015. Seasonal variations of PAHs content and distribution patterns in a mixed land use area: a case study in NE Italy with the transplanted lichen Pseudevernia furfuracea. Atmos. Environ. 113, 255–263.

Kodnik, D., Winkler, A., Candotto Carniel, F., Tretiach, M., 2017. Biomagnetic moni-toring and element content of lichen transplants in a mixed land use area of NEItaly. Sci. Total Environ. 595, 858–867.

Lipowsky, H., Arpaci, E., 2007. Copper in the Automotive Industry. WILEY-VCH Verlag GmbH & Co. KGaA, Weinheim, Germany, 179.

Loppi, S., Ravera, S., Paoli, L., 2019. Coping with uncertainty in the assessment of atmospheric pollution with lichen transplants. Environ. Forensic https://doi.org/10.1080/15275922.2019.1627615.

Lu, S.G., Chen, Y.Y., Shan, H.D., Bai, S.Q., 2009. Mineralogy and heavy metal leachability of magnetic fractions separated from some Chinese coal fly ashes. J. Hazard. Mater. 169 (1–3), 246–255. https://doi.org/10.1016/j.jhazmat.2009.03.078.

Lucadamo, L., Corapi, A., Loppi, S., De Rosa, R., Barca, D., Vespasiano, G., Gallo, L., 2015. Spatial variation in the accumulation of elements in thalli of the lichen Pseudevernia furfuracea (L.) Zopf transplanted around a biomass power plant in Italy. Arch. Environ. Contam. Toxicol. 70 (3), 1–16. https://doi.org/10.1007/s00244-015-0238-4.

Magiera, T., Jabłońska, M., Strzyszcz, Z., Rachwał, M., 2011. Morphological and mineralogical forms of technogenic magnetic particles in industrial dusts. Atmos. Environ. 45, 4281–4290.

Magiera, T., Gołuchowska, B., Jabłońska, M., 2013. Technogenic magnetic particles in alkaline dusts from power and cement plants. Water Air Soil Pollut. 224, 1389.

Maher, B.A., Moore, C., Matzka, J., 2008. Spatial variation in vehicle-derived metal pollution identified by magnetic and elemental analysis of roadside tree leaves. Atmos. Environ. 42, 364–373.

Maher, B.A., Ahmed, I.A.M., Karloukovski, V., MacLaren, D.A., Foulds, P.G., Allsop, D., Mann, D.M.A., Torres-Jardòn, R., Calderon-Garciduenas, L., 2016. Magnetite pollution nanoparticles in the human brain. P Natl Acad Sci USA 113 (39), 10797–10801.

Marié, D.C., Chaparro, M.A.E., Irurzun, M.A., Lavornia, J.M., Marinelli, C., Cepeda, R., Böhnel, H.N., Castañeda Miranda, A.G., Sinito, A.M., 2016. Magnetic mapping of air pollution in Tandil city (Argentina) using the lichen Parmotrema pilosum as biomonitor. Atmospheric Pollution Research 7, 513–520.

Mejía-Echeverry, D., Chaparro, M.A.E., Duque-Trujillo, J.F., Chaparro, M.A.E., Castañeda Miranda, A.G., 2018. Magnetic biomonitoring as a tool for assessment of air pollution patterns in a tropical valley using Tillandsia sp. Atmosphere 9, 283.

Mitchell, R., Maher, B.A., Kinnersley, R., 2010. Rates of particulate pollution deposition onto leaf surfaces: temporal and inter-species magnetic analyses. Environ. Pollut. 158, 1472–1478.

Moreno, E., Sagnotti, L., Dinarès-Turell, J., Winkler, A., Cascella, A., 2003. Biomonitoring of traffic air pollution in Rome using magnetic properties of tree leaves. Atmos. Environ. 37, 2967–2977.

Muhammad, S., Wuyts, K., Samson, R., 2019. Atmospheric net particle accumulation on 96 plant species with contrasting morphological and anatomical leaf characteristics in a common garden experiment. Atmos. Environ. 202, 328–344. https://doi.org/10.1016/j.atmosenv.2019.01.015.

Muxworthy, A.R., Schmidbauer, E., Petersen, N., 2002. Magnetic properties and Mössbauer spectra of urban atmospheric particulate matter: a case study from Munich, Germany. Geophys. J. Int. 150 (2), 558–570.

Nascimbene, J., Tretiach, M., Corana, F., Lo Schiavo, F., Kodnik, D., Dainese, M., Mannucci, B., 2014. Patterns of traffic polycyclic aromatic hydrocarbon pollution in mountain areas can be revealed by lichen biomonitoring: a case study in the Dolomites (Eastern Italian Alps). Sci. Total Environ. 475, 90–96.

Nash III, T.H., 2008. Nutrients, elemental accumulation, mineral cycling. In: Nash III, T.H. (Ed.), Lichen Biology, 2nd ed. Cambridge University Press, Cambridge, UK, pp. 236–253.

Nieboer, E., Richardson, D.H.S., Tomassini, F.D., 1978. Mineral uptake and release by lichens: an overview. Bryologist 81, 226–246.

Nimis, P.L., Bargagli, R., 1999. Linee-guida per l'utilizzo di licheni epifiti come bioaccumulatori di metalli in traccia. In: Piccini, C., Salvati, S. (Eds.), Atti del Workshop Biomonitoraggio della qualità dell'aria sul territorio nazionale. Roma 26–27 Novembre 1998. ANPA, Serie Atti 2/1999, Roma. pp. 279–289.

Nimis, P.L., Lazzarin, G., Lazzarin, A., Skert, N., 2000. Biomonitoring of trace element with lichens in Veneto. Sci. Total Environ. 255, 97–111.

Owczarek, M., Guidotti, M., Blasi, G., De Simone, C., De Marco, A., 2001. Traffic pollution monitoring using lichenes as bioaccumulators of heavy metals and PAH. Fresenjus Environm. Bull. 10 (1), 42–45.

Paoli, L., Winkler, A., Guttová, A., Sagnotti, A., Grassi, A., Lackovičová, A., Senko, D., Loppi, S., 2017. Magnetic properties and element concentrations in lichens exposed to airborne pollutants released during cement production. Environ. Sci. Pollut. Res. 24 (13), 12063–12080. https://doi.org/10.1007/s11356-016-6203-6.

Paoli, L., Vannini, A., Fa˘ckovcová, Z., Guarnieri, M., Ba˘ckor, M., Loppi, S., 2018. One year of transplant: is it enough for lichens to reflect the new atmospheric conditions?. Ecol. Indic. 88, 495–502.

Protano, C., Guidotti, M., Owczarek, M., Fantozzi, L., Blasi, G., Vitali, M., 2014. Polycyclic aromatic hydrocarbons and metals in transplanted lichen (Pseudovernia furfuracea) at sites adjacent to a solidwaste landfill in Central Italy. Arch. Environ. Contam. Toxicol. 66, 471–481. https://doi.org/10.1007/s00244-013-9965-6.

Protano, C., Owczareck, M., Antonucci, A., Guidotti, M., Vitali, M., 2017. Assesting indoor air quality of school environments: transplanted lichen Pseudovenia furfuracea as a new tool for biomonitoring and bioaccumulation. Environ. Monit. Assess. 189–358.

Quevauviller, P., Herzig, R., Muntau, H., 1996. Certified reference material of lichen (CRM 482) for the quality control of trace element biomonitoring. Sci. Total Environ. 187, 143–152.

Rachwał, M., Rybak, J., Rogula-Kozłowska, W., 2018. Magnetic susceptibility of spider webs as a proxy of airborne metal pollution. Environ. Pollut. 234, 543–551. https://doi.org/10.1016/j.envpol.2017.11.088, (Epub 2017 Dec 21).

Rai, P.K., 2013. Environmental magnetic studies of particulates with special reference to biomagnetic monitoring using roadside plant leaves. Atmos. Environ. 72, 113–129.

Revuelta, M.A., McIntosh, G., Pey, J., Pérez, N., Querol, X., Alastuey, A., 2014. Partitioning of magnetic particles in PM_{10}, $PM_{2.5}$ and PM_1 aerosols in the urban atmosphere of Barcelona (Spain). Environ. Pollut. 188, 109–117.

Roberts, A.P., Tauxe, L., Heslop, D., Zhao, X., Jiang, Z., 2018. A critical appraisal of the 'Day' diagram. Journal of Geophysical Research: Solid Earth 123, 2618–2644. https://doi.org/10.1002/2017JB015247.

Sagnotti, L., Winkler, A., 2012. On the magnetic characterization and quantification of the superparamagnetic fraction of traffic-related urban airborne PM in Rome, Italy. Atmos. Environ. 59, 131–140. https://doi.org/10.1016/j.atmosenv.2012.04.058.

Sagnotti, L., Taddeucci, J., Winkler, A., Cavallo, A., 2009. Compositional, morphological, and hysteresis characterization of magnetic airborne particulate matter in Rome, Italy. Geochem Geophy Geosy 10, https://doi.org/10.1029/2009GC002563.

Salo, H., Mäkinen, J., 2014. Magnetic biomonitoring by moss bags for industry-derived air pollution in SW Finland. Atmos. Environ. 97, 19–27.

Salo, H., Bućko, M.S., Vaahtovuo, E., Limo, J., Mäkinen, J., Pesonen, L.J., 2012. Biomonitoring of air pollution in SW Finland by magnetic and chemical measurements of moss bags and lichens. J. Geochem. Explor. 115, 69–81.

Sarbak, Z., Stanczyk, A., Kramer-Wachowiak, M., 2004. Characterization of surface properties of various fly ashes. Powder Technol. 145, 82–87. https://doi.org/10.1016/j.pow-tec.2004.04.041.

Szönyi, M., Sagnotti, L., Hirt, A.M., 2007. On leaf magnetic homogeneity in particulate matter biomonitoring studies. Geophys. Res. Lett. 34, https://doi.org/10.1029/2006GL029076.

Szönyi, M., Sagnotti, L., Hirt, A.M., 2008. A refined biomonitoring study of airborne particulate matter pollution in Rome, with magnetic measurements on Quercus ilex tree leaves. Geophys. J. Int. 173, 127–141.

Tomlinson, D.L., Wilson, J.G., Harris, C.R., Jeffrey, D.W., 1980. Problems in the assessment of heavy-metal levels in estuaries and the formation of a pollution index. Helgol. Meeresunters 33, 566–575.

Tretiach, M., Crisafulli, P., Pittao, E., Rinino, S., Roccotiello, E., Modenesi, P., 2005. Isidia ontogeny and its effects on the CO_2 gas exchanges of the epiphytic lichen Pseudevernia furfuracea (L.) Zopf. Lichenologist 37, 445–462.

Tretiach, M., Adamo, P., Bargagli, R., Baruffo, L., Carletti, L., Crisafulli, P., Giordano, S., Modenesi, P., Orlando, S., Pittao, E., 2007. Lichen and moss bags as monitoring devices in urban areas. Part I: influence of exposure on sample vitality. Environ. Pollut. 146, 380–391.

Tretiach, M., Candotto Carniel, F., Loppi, S., Carniel, A., Bortolussi, A., Mazzilis, D., Del Bianco, C., 2011. Lichen transplants as a suitable tool to identify mercury pollution from waste incinerators: a case study from NE Italy. Environ. Monit. Assess. 175, 589–600.

Veneva, L., Hoffmann, V., Jordanova, D., Jordanova, N., Fehr, T., 2004. Rock magnetic, mineralogical and micro-structural characterization of fly ashes from Bulgarian power plants and the nearby anthropogenic soils. Phys. Chem. Earth 29, 1011–1023.

Vingiani, S., Adamo, P., Giordano, S., 2004. Sulphur, nitrose and carbon contento of Sphagnum capillifolium and Pseudevernia furfuracea exposed in bags in the Naples urban area. Environ. Pollut. 129 (1), 145–158.

Vuković, G., Aničić Urošević, M., Tomašević, M., Samson, R., Popović, A., 2015. Biomagnetic monitoring of urban air pollution using moss bags (Sphagnum girgensohnii). Ecol. Indic. 52, 40–47.

Wang, X., Løvlie, R., Zhao, X., Yang, Z., Jiang, F., Wang, S., 2010. Quantifying ultrafine pedogenic magnetic particles in Chinese loess by monitoring viscous decay of superparamagnetism. Geochem. Geophys. Geosyst. 11, https://doi.org/10.1029/2010GC003194.

WHO (World Health Organization), 2014. Fact sheet N°313: ambient (outdoor) air quality and health. In: http://www.who.int/mediacentre/factsheets/fs313/en/.

WHO (World Health Organization), 2016. http://www.who.int/gho/phe/outdoor_air_pollution/en/, (last visit 8th February 2016).

Wolterbeek, H.T., Bode, P., 1995. Strategies in sampling and sample handling in the context of large-scale plant biomonitoring surveys of trace element air pollution. Sci. Total Environ. 176, 33–43.

Zhang, C., Huang, B., Li, Z., Liu, H., 2006. Magnetic properties of high-road-side pine tree leaves in Beijing and their environmental significance. Chin. Sci. Bull. 51, 3041–3052.

Zhang, C., Huang, B., Piper, J.D.A., Luo, R., 2008. Biomonitoring of atmospheric particulate matter using magnetic properties of Salix matsudana tree ring cores. Sci. Total Environ. 393, 177–190.

Zhu, Z., Li, Z., Bi, X., Han, Z., Yu, G., 2013. Response of magnetic properties to heavy metal pollution in dust from three industrial cities in China. J. Hazard. Mater. 246–247, 189–198. https://doi.org/10.1016/j.jhazmat.2012.12.024.